A Ka-Band Broadband Integrated Transition of Air-Filled Waveguide to Laminated Waveguide

Xiaobo Huang and Ke-Li Wu, *Fellow, IEEE*

***Abstract*—In this letter, a novel compact and broadband integrated transition between a laminated waveguide and an air-filled rectangular waveguide operating in Ka band is proposed. A three-pole filter equivalent circuit model is employed to interpret the working mechanism and to predict the performance of the transition. A back-to-back prototype of the proposed transition is designed and fabricated for proving the concept. Good agreement of the measured and simulated results is obtained. The measured result shows that the insertion loss of better than 0.26 dB from 34.8 to 37.8 GHz can be achieved.**

***Index Terms*—Broadband, laminated waveguide, LTCC, millimeter wave, transitions.**

I. Introduction

OWING to its unique low loss characteristic, waveguide transmission line is usually the first choice for transmitting millimeter wave signals. Instead of using traditional solid metal waveguide, the concept of laminated waveguide [1], [2] was proposed for implementing a waveguide circuit by a planar laminated substrate. The cross-sectional size of the laminated waveguide can be significantly reduced by using a high dielectric constant substrate. The concept has been further extended to a multi-layered printed circuit boards (PCB) and has been called substrate integrated waveguide (SIW) [3].

In many applications, it is frequently seen that an integrated laminated waveguide system needs to be interfaced with an external system whose interface port is an air-filled waveguide. In this scenario, a key component for connecting the two different types of modules is a transition of an air-filled waveguide to laminated waveguide. Many configurations have been reported on transitions between laminated waveguide and a commonly-used transmission line, such as microstrip, stripline [3], [4] and coplanar waveguide [5]. Some works have been reported on a transition between air-filled and laminated waveguides. An earlier work of such transitions employed a pair of two-pole bandpass filters to create two reflection zeros in the pass-band [6]. Another work used a bulky waveguide taper between SIW and air-filled waveguide [7].

In this letter, a novel compact and broadband transition between an air-filled waveguide and a laminated waveguide is proposed. The concept is proven at Ka band by an LTCC based prototyping module. A three-pole filter circuit model with cross couplings is proposed to explain its working principle, by which three reflection zeros within the pass band are created. The proposed transition uses a completely different design concept from that in [6] to create three coupled resonators along the long side of the air-waveguide. The new configuration occupies minimum space for a wideband transition. It will be seen that the new transition takes only half of the area as that the previous structure in [6] would take by taking advantage of the limited volume in substrate near the air-waveguide aperture. To verify the proposed transition configuration and validate the circuit model, a back-to-back transition prototype is designed, fabricated and tested. Good agreement of the measured and the simulated results is achieved.

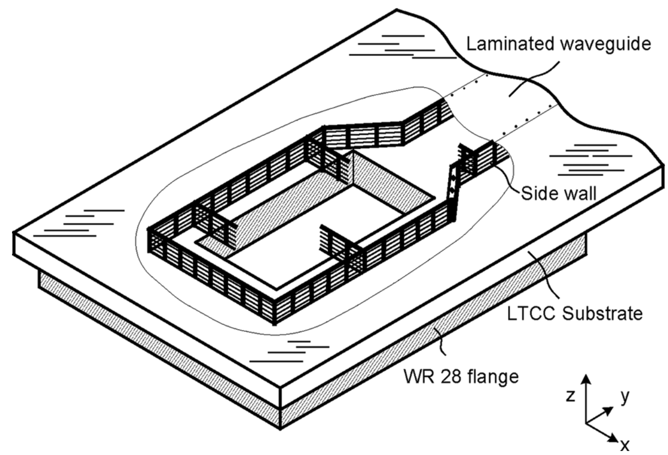

Fig. 1. Structure of the proposed air-filled waveguide to laminated waveguide transition.

II. Configuration and Working Mechanism

Fig. 1 illustrates a perspective cut-away view of the proposed structure. The top and bottom layers of the module are covered by metal surface except the rectangular aperture, which has the same inner dimensions as that of the air-filled waveguide and is defined as an input port of the transition module.Correspondingly, the cross-sectional aperture at the end of laminated waveguide is defined as output port. As shown in Fig. 2, the four interior stubs perpendicularly connected to the side walls divide the interior compartment into three coupled resonators denoted as 1, 2 and 3. The three resonators are excited in phase by the input aperture and are in-line coupled through the windows between each pair of stubs.

A. Role of the Interior Stubs and Conversion of TE_{10} Modes

In principle, the four alternately inserted stubs create three quasi-half-wavelength resonators in the LTCC substrate partially bounded by the interface between the air and the high

Manuscript received July 10, 2012; accepted September 02, 2012. Date of publication September 20, 2012; date of current version October 03, 2012.

The authors are with the Department of Electronic Engineering, The Chinese University of Hong Kong, Shatin, Hong Kong, China (e-mail: xbhuang@ee.cuhk.edu.hk; klwu@ee.cuhk.edu.hk).

Color versions of one or more of the figures in this letter are available online at http://ieeexplore.ieee.org.

Digital Object Identifier 10.1109/LMWC.2012.2218095

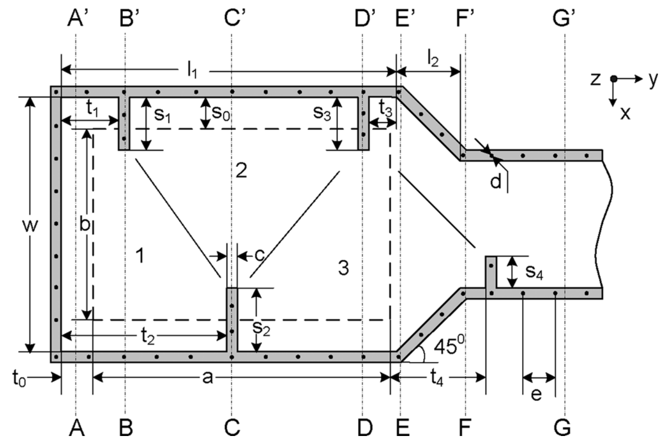

Fig. 2. Top view of the proposed transition and division of the three resonators.

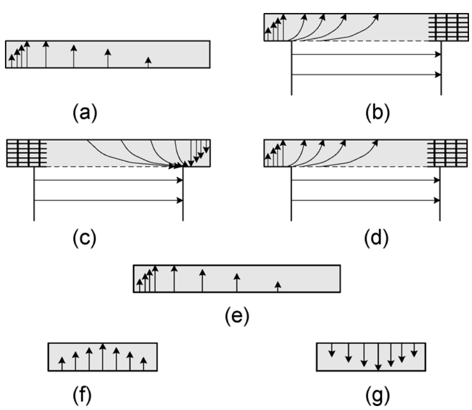

Fig. 3. Electric field lines in the proposed transition at the plane of: (a) A-A'; (b) B-B'; (c) C-C'; (d) D-D'; (e) E-E'; (f) F-F'; (g) G-G'.

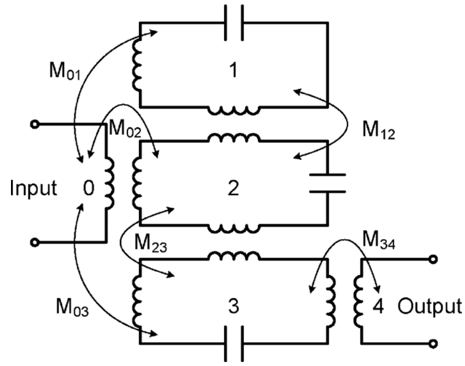

Fig. 4. Equivalent circuit model of the proposed transition.

dielectric constant LTCC substrate. In order to demonstrate the conversion of the TE_{10} mode across the air-filled waveguide to the TE_{10} mode at the laminated waveguide port, the electric field lines at the reference planes of A-A' to G-G' in Fig. 2 of a designed transition are illustrated in Fig. 3.

B. Equivalent Circuit Model

Obviously, an operating transition can be regarded as a three-pole bandpass filter. Thus, the concept of filter design can be employed to explain the working mechanism and design guidelines of the proposed transition. Based on the physical coupling arrangement, the equivalent circuit model shown in Fig. 4 is proposed to predict the performance of the transition, in which each *LC* loop represents the corresponding resonator in the transition structure. The coupling coefficients, M_{01}, M_{02} and M_{03}, denote the couplings between air-filled waveguide port and the three resonators through the input aperture, respectively, and the coupling coefficient M_{34} stands for the coupling between the laminated waveguide port and Resonator 3. The coupling coefficients M_{12} and M_{23} signify the mutual couplings between the three resonators. According to the equivalent circuit, there will be three reflection zeros within the pass-band and two transmission zeros in the finite frequency region if the coupling matrix is appropriately designed. Note that two transmission zeros are introduced by cross coupling M_{03}.

III. Design Procedure

To illustrate the design procedure, an air-filled waveguide to an LTCC laminated waveguide transition working at 36.3 GHz is designed. The Ansoft HFSS electromagnetic (EM) simulation software is used for simulating the physical structure. A 3 mm long air-filled waveguide and a section of 2.5 mm long laminated waveguide are incorporated in the design model. The substrate tape adopted is Ferro M6 with manufacturer specified dielectric constant of 6.1 and loss tangent of 0.002. The height of the laminated waveguide is 0.66 mm composing of 6 layers of LTCC tapes. As a matter of fact, the three inter-coupled resonators shown in Fig. 2 are constructed by analogously triangular laminated cavities. The resonant modes in the cavities are excited by the TE_{10} mode in phase at the air-filled waveguide. The eigen mode solver of HFSS can be used to obtain the initial dimensions of each resonator. It can be seen that the input couplings are mainly controlled by the position of the input aperture, while the mutual couplings between resonators and the output coupling vary with the length of the four stubs. The related dimensional variables of the transition are given in Fig. 2.

With the coupled resonator circuit model representation given in Fig. 4, the corresponding coupling matrix for the desired pass-band performance can be obtained by a classical filter synthesis procedure [8] and is given here with $M_{01} = 0.6651$, $M_{02} = -0.4779$, $M_{03} = 0.7774$, $M_{11} = -0.8596$, $M_{12} = -0.7724$, $M_{22} = 0.8661$, $M_{23} = 0.5585$, $M_{33} = -0.1556$, and $M_{34} = 1.1233$. The transmission zeros prescribed are located at -1.6 and 1.25 on the imaginary axis in the low-pass filter prototype. It is noted that M_{02} is with a negative sign to reflect the opposite electric field polarization in Resonator 2 as compared to that in Resonators 1 and 3. Although the center frequency and bandwidth used in circuit model synthesis are 36.3 GHz and 3 GHz, respectively, the same coupling matrix can be scaled to other frequency and bandwidth.

With appropriate initial design, a few more steps of fine tuning can be performed on those critical variables by a method of computer aided tuning. The computer aided diagnosis and tuning lead the design solution to the one specified by the synthesized circuit model. This statement is justified by a closed correlation of the synthesized coupling coefficients with those of the extracted from the final physical design, which are $M_{01} = 0.6558$, $M_{02} = -0.4774$, $M_{03} = 0.7769$, $M_{11} = -0.8586$, $M_{12} = -0.7731$, $M_{22} = 0.8661$, $M_{23} = 0.5591$, $M_{33} = -0.1567$ and $M_{34} = 1.1234$. The detailed dimensions of an optimized transition are given in Table I. The simulated frequency responses of the EM model and that of the equivalent circuit model are superimposed in Fig. 5. The EM simulated results reveal that the single transition

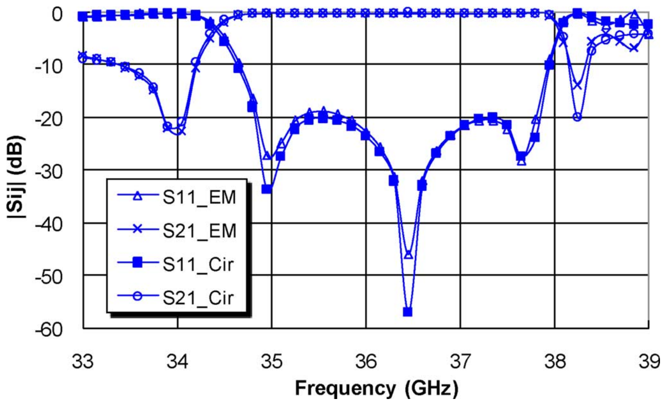

Fig. 5. Scattering parameters of the EM and circuit models of the single transition design example.

TABLE I
DIMENSIONS OF THE SINGLE TRANSITION DESIGN EXAMPLE.

Variables	Size (mm)	Variables	Size (mm)	Variables	Size (mm)
a	7.11	l_1	7.72	s_4	0.60
b	3.56	l_2	0.78	t_0	0.51
c	0.24	s_0	0.43	t_1	0.64
d	0.17	s_1	1.10	t_2	3.64
e	0.60	s_2	1.10	t_3	0.71
w	4.41	s_3	1.20	t_4	1.82

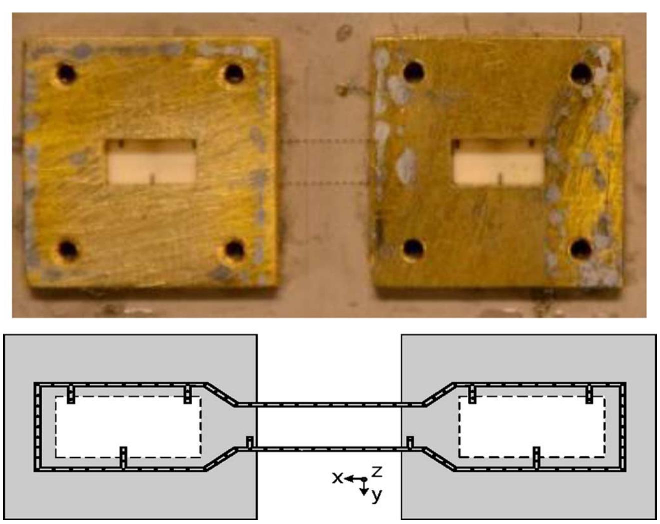

Fig. 6. Photo of the back-to-back test module and its structure illustration.

has an impedance matching bandwidth of 3 GHz with 20 dB return loss and less than 0.25 dB insertion loss across the operating frequency band.

Owing to different waveguide interfaces at the two ports, it is difficult to experimentally characterize the performance of a single transition. Therefore, a back-to-back test module of the proposed transition on an LTCC substrate is fabricated and tested. A photo of the test module and its structure illustration is shown in Fig. 6, in which the length of the laminated waveguide between two transitions is 14.4 mm. The measured and the EM simulated S-parameters are shown in Fig. 7. It should be mentioned that waveguide TRL calibration was used to define the reference plane right at the waveguide-LTCC interface.

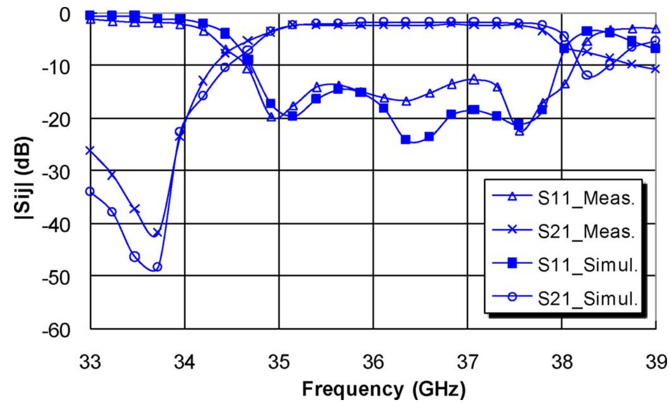

Fig. 7. Measured and the simulated S-parameters of the back-to-back verification LTCC module.

The measured in band insertion loss of the back-to-back module is better than 1.3 dB from 34.8–37.8 GHz with a return loss better than 13 dB. Considering that the simulated insertion loss of the 14.4 mm long laminated waveguide is about 0.6 dB and that the extra insertion loss of 0.18 dB is caused by the 13 dB return loss (against a 20 dB return loss), it can be derived that the measured insertion loss of a single transition would be about 0.26 dB, which matches to the EM simulated result very well.

IV. CONCLUSION

A novel compact and broadband integrated transition between an air-filled waveguide and a laminated waveguide is proposed. Good agreement is achieved between the simulated and measured results, which verifies the performance of the transition and validates the circuit model. The proposed transition provides many attractive features with excellent performance in terms of its compact size, wide bandwidth and convenience to be integrated with other planar circuits.

ACKNOWLEDGMENT

The authors wish to thank Dr. Y. Huang and Dr. J. Wang, (SuZhou) Bohai Microsystem, Inc., for their suuport, valuable advice, and generous help in LTCC module prototyping.

REFERENCES

[1] F. Shigeki, "Waveguide Line," Japan Patent 06-053 711, Feb. 25, 1994.
[2] H. Uchimura, T. Takenoshita, and M. Fujii, "Development of a laminated waveguide," *IEEE Trans. Microw. Theory Tech.*, vol. 46, no. 12, pp. 2438–2443, Dec. 1998.
[3] D. Deslandes and K. Wu, "Integrated microstrip and rectangular waveguide in planar form," *IEEE Microw. Wireless Compon. Lett.*, vol. 11, no. 2, pp. 68–70, Feb. 2001.
[4] Y. Ding and K. Wu, "Substrate integrated waveguide-to-microstrip transition in multilayer substrate," *IEEE Trans. Microw. Theory Tech.*, vol. 55, no. 12, pp. 2839–2844, Dec. 2007.
[5] S. H. Lee, S. W. Jung, and H. -Y. Lee, "Ultra-wideband CPW-to-substrate integrated waveguide transition using an elevated-CPW section," *IEEE Microw. Wireless Compon. Lett.*, vol. 18, no. 11, pp. 746–748, Nov. 2008.
[6] Y. Huang and K.-L. Wu, "A broadband LTCC integrated transition of laminated waveguide to air-filled waveguide for millimeter wave applications," *IEEE Trans. Microw. Theory Tech.*, vol. 51, no. 5, pp. 1613–1617, May 2003.
[7] L. Xia, R. Xu, B. Yan, J. Li, Y. Guo, and J. Wang, "Broadband transition between air-filled waveguide and substrate integrated waveguide," *Electron. Lett.*, vol. 42, no. 24, pp. 1403–1405, Nov. 2006.
[8] R. J. Cameron, "General coupling matrix synthesis methods for Chebyshev filtering functions," *IEEE Trans. Microw. Theory Tech.*, vol. 47, no. 4, pp. 433–442, Apr. 1999.